IEICE TRANS. ELECTRON., VOL.E100–C, NO.1 JANUARY 2017

PAPER

Increase of Recognizable Label Number with Optical Passive Waveguide Circuits for Recognition of Encoded 4- and 8-Bit BPSK Labels

Hiroki KISHIKAWA[†a)], ***Member***, **Akito IHARA**[†*], ***Nonmember***, **Nobuo GOTO**[†], ***Senior Member***, ***and*** **Shin-ichiro YANAGIYA**[†], ***Nonmember***

SUMMARY Optical label processing is expected to reduce power consumption in label switching network nodes. Previously, we proposed passive waveguide circuits for the recognition of BPSK labels with a theoretically infinite contrast ratio. The recognizable label number was limited to four and eight for 4-bit and 8-bit BPSK labels, respectively. In this paper, we propose methods to increase the recognizable label number. The proposed circuits can recognize eight and sixteen labels of 4-bit BPSK codes with a contrast ratio of 4.00 and 2.78, respectively. As 8-bit BSPK codes, 64, 128, and 256 labels can be recognized with a contrast ratio of 4.00, 2.78, and 1.65, respectively. In recognition of all encoded labels, that is, 16 and 256 labels for 4-bit and 8-bit BPSK labels, a reference signal is employed to identify the sign of the optical output signals. The effect of phase deviation and loss along the optical waveguides of the devices is also discussed.

key words: *code recognition, optical waveguide circuits, optical BPSK code*

1. Introduction

Optical encoded labels have been employed to carry information in label-routed photonic networks [1], [2]. Optical processing for labels which are not converted to electrical signals is expected to reduce electrical power consumption in network nodes. Binary phase-shift-keying (BPSK) codes are one of the basic formats for the optical labels as well as for optical payload. Optical correlator-based systems have been investigated to recognize matched labels, which include systems consisting of fiber Bragg grating [3], taps and delay lines [2], and combination of a grating and spatial filters [4]–[6]. Multiple labels that correspond to a partial set of binary codes have also been recognized with waveguide-type circuits consisting of arrayed waveguide gratings (AWGs) [7], [8] and cascaded interferometers [9], [10].

We have proposed a passive waveguide circuit to recognize all BPSK coded labels [11], [12]. The device consists of a tree-structure connection of asymmetric X-junction couplers [13]. The number of the output ports for N-bit labels is 2^N. The contrast ratio, which is expressed as the ratio of the largest intensity at the desired output port corresponding to the incident label to the secondly largest intensity among other ports, is 2.78 and 1.65 for $N = 4$ and 8, respectively [12]. We also proposed another recognition circuit for a partial set of the binary codes, which provides an infinite contrast ratio [14]. In this paper, we investigate the increase in the number of recognizable labels with waveguide circuits based on the latter circuit. A basic idea to increase the number of recognizable 4-bit BPSK labels was also briefly discussed in [14]. In this paper, we discuss systematically how to increase the number of available labels for 4- and 8-bit binary codes and find optimum circuit parameters. It is shown that the number of recognizable labels can be increased at the expense of decreasing the contrast ratio. However, the decrease of the contrast ratio can be suppressed by limiting employed labels to a set of classified labels. Therefore, the obtained results will give useful information to design a set of labels which meet requirement for a minimum contrast ratio at the output.

We also clarify the effect of phase deviation along waveguides and propagation loss variation between waveguides, which gives allowable fabrication error for the optical waveguide device only consisting of optical passive elements.

The remainder of this paper is organized as follows: Sect. 2 gives brief description of the basic optical waveguide circuits for the recognition of 4-bit and 8-bit labels. In Sect. 3, we discuss methods to increase the recognizable labels by extending the circuits for 4-bit labels. In Sect. 4, we apply similar methods to 8-bit labels. The results are discussed in comparison with tree-structure waveguide circuits [12] in Sect. 5. In Sect. 6, conclusions are presented.

2. Basic Waveguide Circuits for 4- and 8-Bit Label Recognition

A basic waveguide circuit for the recognition of four 4-bit BPSK labels is shown in Fig. 1 [14]. The device consists of four asymmetric X-junction couplers, X_i, $i = 1, \ldots, 4$, and interconnecting waveguides. The phases ϕ_i and the transmission coefficients β_i, $i = 1, \ldots, 4$, mean the phase deviations due to model fabrication error and the attenuations due to propagation loss or scattering in the waveguides, respectively. Note that, in ideal devices, these phase deviations

Manuscript received March 31, 2016.
Manuscript revised August 23, 2016.

[†]The authors are with Department of Optical Science and Technology, Tokushima University, Tokushima-shi, 770–8506 Japan.
[*]Presently, with Fujitsu Systems West Ltd.
a) E-mail: kishikawa.hiroki@tokushima-u.ac.jp

DOI: 10.1587/transele.E100.C.84

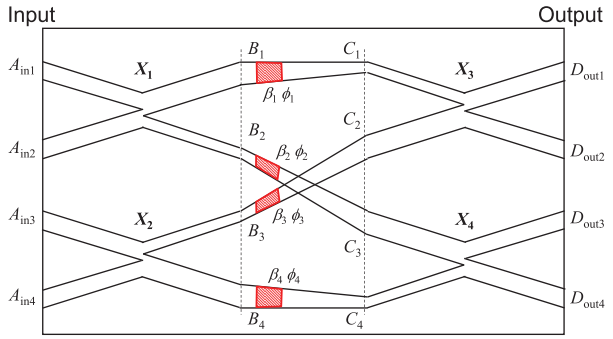

Fig. 1 A basic optical waveguide circuit for the recognition of the 4-bit BPSK labels.

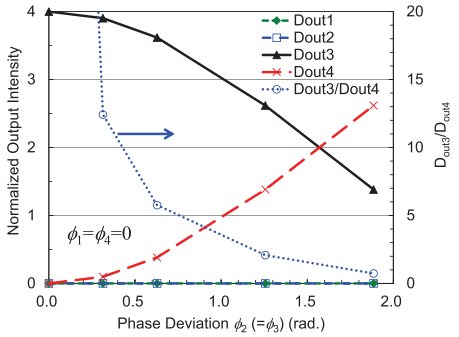

Fig. 2 The output intensities as a function of the phase deviation ϕ_2 (= ϕ_3) for the 4-bit basic module.

ϕ_i are 0 and β_i are equal to one. An optical 4-bit label is supposed to have been converted from a serial pulse train to parallel pulses with a preprocessor. The parallel pulses are input in the input ports at the same time. We denote $\beta_i e^{j\phi_i}$ as α_i. The output optical fields $D_{\text{out}\,j}$, $j = 1, \ldots, 4$, are related to the input fields $A_{\text{in}\,i}$, $i = 1, \ldots, 4$, as [14]

$$\begin{pmatrix} D_{\text{out1}} \\ D_{\text{out2}} \\ D_{\text{out3}} \\ D_{\text{out4}} \end{pmatrix} = \frac{1}{2} \begin{pmatrix} \alpha_1 & \alpha_1 & \alpha_3 & -\alpha_3 \\ -\alpha_1 & -\alpha_1 & \alpha_3 & -\alpha_3 \\ -\alpha_2 & \alpha_2 & -\alpha_4 & -\alpha_4 \\ -\alpha_2 & \alpha_2 & \alpha_4 & \alpha_4 \end{pmatrix} \begin{pmatrix} A_{\text{in1}} \\ A_{\text{in2}} \\ A_{\text{in3}} \\ A_{\text{in4}} \end{pmatrix}. \tag{1}$$

We consider four BPSK labels $\boldsymbol{A}_i^{(1)}$, $i = 1, \ldots, 4$, as defined by

$$\begin{aligned} \left(\boldsymbol{A}_1^{(1)} \;\; \boldsymbol{A}_2^{(1)} \;\; \boldsymbol{A}_3^{(1)} \;\; \boldsymbol{A}_4^{(1)} \right) &= \left(\boldsymbol{A}_1 \;\; \boldsymbol{A}_2 \;\; \boldsymbol{A}_3 \;\; \boldsymbol{A}_4 \right) \\ &= \begin{pmatrix} 1 & -1 & 1 & 1 \\ -1 & 1 & 1 & 1 \\ 1 & 1 & 1 & -1 \\ 1 & 1 & -1 & 1 \end{pmatrix}, \end{aligned} \tag{2}$$

where $\boldsymbol{A}_i$ is a column vector of optical field and the superscript (1) denotes the 4-bit labels. The output fields $\boldsymbol{D}_i^{(1)}$ for $\boldsymbol{A}_i^{(1)}$ is obtained from Eqs. (1) and (2) as

$$\begin{aligned} &\left(\boldsymbol{D}_1^{(1)} \;\; \boldsymbol{D}_2^{(1)} \;\; \boldsymbol{D}_3^{(1)} \;\; \boldsymbol{D}_4^{(1)} \right) \\ &= \begin{pmatrix} 0 & 0 & \alpha_1 + \alpha_3 & \alpha_1 - \alpha_3 \\ 0 & 0 & -\alpha_1 + \alpha_3 & -\alpha_1 - \alpha_3 \\ -\alpha_2 - \alpha_4 & \alpha_2 - \alpha_4 & 0 & 0 \\ -\alpha_2 + \alpha_4 & \alpha_2 + \alpha_4 & 0 & 0 \end{pmatrix}. \end{aligned} \tag{3}$$

Although each input label has an output with an infinite contrast ratio for the ideal case of $\alpha_i = 1$, the number of the recognizable labels is limited to four.

We now consider the effect of phase deviation ϕ_i with $\beta_i = 1$. Figure 2 shows the output intensities as a function of ϕ_2 (= ϕ_3), whereas $\phi_1 = \phi_4 = 0$ is assumed. Since the asymmetric X-junction coupler discriminates a phase difference π between the two inputs, the outputs from D_{out1} and D_{out2} are reversed at $\phi_2 = \phi_3 = \pi$. The ratio of $D_{\text{out3}}/D_{\text{out4}}$ is also plotted to evaluate the contrast ratio. It is found that the deviation at the output intensities is kept below 2.5 % of the maximum output when the phase deviation is less than 0.1π rad, resulting in a contrast ratio larger than 12.4.

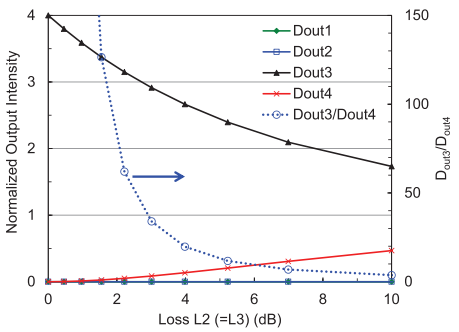

Fig. 3 The output intensities as a function of waveguide loss L_2 (= L_3) for the 4-bit basic module, where the other losses and the phase deviation is assumed to be 0.

Next, we consider the effect of waveguide loss. Since the crossed waveguides are expected to have larger scattering loss, we evaluate the output as a function of L_2 (= L_3), whereas $L_1 = L_4 = 0$. Here, we define $L_i = -10\log_{10}\beta_i$. Figure 3 shows the calculated results. Loss of $L_2 = L_3 = 2.2$ dB, which corresponds to 0.77 of β_2 and β_3, induces a decrease of 21.3 % and an increase relative to D_{out3} of 1.3 % at D_{out3} and D_{out4}, respectively. The contrast ratio decreases from infinity to 62.0.

In addition to scattering and crosstalk at the crossed waveguides, the asymmetric X-junction coupler may induce scattering. Although the coupling performance of the asymmetric X-junction coupler does not have large dependence on the waveguide widths and the crossed angle, edge roughness of the waveguide at the junction induces scattering. Such fabrication error and roughness induce imbalance splitting, resulting in the degradation of the output contrast ratio.

The basic waveguide circuit for the 4-bit label recognition can be scaled to the 8-bit label recognition as shown in Fig. 4 [14]. The circuit consists of two 4-bit basic modules shown in Fig. 1 and four asymmetric X-junction couplers at the outputs. The transmission coefficients, β_{1i} and β_{2i}, and the phase deviations, ϕ_{1i} and ϕ_{2i}, correspond to β_i and ϕ_i in the basic module of Fig. 1, respectively. The output

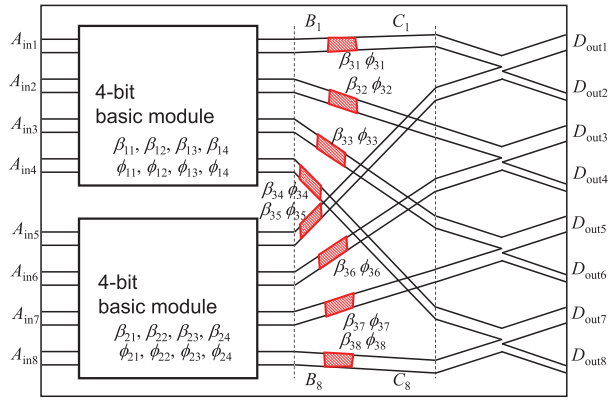

Fig. 4 A basic optical waveguide circuit for the recognition of the 8-bit BPSK labels.

fields $D_{\text{out}\,j}$, $j = 1, \ldots, 8$ are related to the input fields $A_{\text{in}\,i}$, $i = 1, \ldots, 8$, as

$$\begin{pmatrix} D_{\text{out1}} \\ D_{\text{out2}} \\ \vdots \\ D_{\text{out8}} \end{pmatrix} = T_8 \begin{pmatrix} A_{\text{in1}} \\ A_{\text{in2}} \\ \vdots \\ A_{\text{in8}} \end{pmatrix}, \tag{4}$$

where

$$T_8 = \frac{1}{2\sqrt{2}} \begin{pmatrix} \alpha_{31}\alpha_{11} & \alpha_{31}\alpha_{11} & \alpha_{31}\alpha_{13} & -\alpha_{31}\alpha_{13} \\ -\alpha_{31}\alpha_{11} & -\alpha_{31}\alpha_{11} & -\alpha_{31}\alpha_{13} & \alpha_{31}\alpha_{13} \\ -\alpha_{32}\alpha_{11} & -\alpha_{32}\alpha_{11} & \alpha_{32}\alpha_{13} & -\alpha_{32}\alpha_{13} \\ \alpha_{32}\alpha_{11} & \alpha_{32}\alpha_{11} & -\alpha_{32}\alpha_{13} & \alpha_{32}\alpha_{13} \\ -\alpha_{33}\alpha_{12} & \alpha_{33}\alpha_{12} & -\alpha_{33}\alpha_{14} & -\alpha_{33}\alpha_{14} \\ \alpha_{33}\alpha_{12} & -\alpha_{33}\alpha_{12} & \alpha_{33}\alpha_{14} & \alpha_{33}\alpha_{14} \\ -\alpha_{34}\alpha_{12} & \alpha_{34}\alpha_{12} & \alpha_{34}\alpha_{14} & \alpha_{34}\alpha_{14} \\ \alpha_{34}\alpha_{12} & -\alpha_{34}\alpha_{12} & -\alpha_{34}\alpha_{14} & -\alpha_{34}\alpha_{14} \end{pmatrix}$$

$$\begin{pmatrix} \alpha_{35}\alpha_{21} & \alpha_{35}\alpha_{21} & \alpha_{35}\alpha_{23} & -\alpha_{35}\alpha_{23} \\ \alpha_{35}\alpha_{21} & \alpha_{35}\alpha_{21} & \alpha_{35}\alpha_{23} & -\alpha_{35}\alpha_{23} \\ -\alpha_{36}\alpha_{21} & -\alpha_{36}\alpha_{21} & \alpha_{36}\alpha_{23} & -\alpha_{36}\alpha_{23} \\ -\alpha_{36}\alpha_{21} & -\alpha_{36}\alpha_{21} & \alpha_{36}\alpha_{23} & -\alpha_{36}\alpha_{23} \\ -\alpha_{37}\alpha_{22} & \alpha_{37}\alpha_{22} & -\alpha_{37}\alpha_{24} & -\alpha_{37}\alpha_{24} \\ -\alpha_{37}\alpha_{22} & \alpha_{37}\alpha_{22} & -\alpha_{37}\alpha_{24} & -\alpha_{37}\alpha_{24} \\ -\alpha_{38}\alpha_{22} & \alpha_{38}\alpha_{22} & \alpha_{38}\alpha_{24} & \alpha_{38}\alpha_{24} \\ -\alpha_{38}\alpha_{22} & \alpha_{38}\alpha_{22} & \alpha_{38}\alpha_{24} & \alpha_{38}\alpha_{24} \end{pmatrix}, \tag{5}$$

where $\alpha_{ij} = \beta_{ij} e^{j\phi_{ij}}$.

We consider eight BPSK labels $\boldsymbol{A}_i^{(2)}$, $i = 1, \ldots, 8$, as defined by

$$\begin{pmatrix} \boldsymbol{A}_1^{(2)} & \boldsymbol{A}_2^{(2)} & \boldsymbol{A}_3^{(2)} & \boldsymbol{A}_4^{(2)} & \boldsymbol{A}_5^{(2)} & \boldsymbol{A}_6^{(2)} & \boldsymbol{A}_7^{(2)} & \boldsymbol{A}_8^{(2)} \end{pmatrix} = \begin{pmatrix} \boldsymbol{A}_1 & \boldsymbol{A}_1 & \boldsymbol{A}_2 & \boldsymbol{A}_2 & \boldsymbol{A}_3 & \boldsymbol{A}_3 & \boldsymbol{A}_4 & \boldsymbol{A}_4 \\ \boldsymbol{A}_1 & \bar{\boldsymbol{A}}_1 & \boldsymbol{A}_2 & \bar{\boldsymbol{A}}_2 & \boldsymbol{A}_3 & \bar{\boldsymbol{A}}_3 & \boldsymbol{A}_4 & \bar{\boldsymbol{A}}_4 \end{pmatrix}, \tag{6}$$

where $\bar{\boldsymbol{A}}_i = -\boldsymbol{A}_i$ and the superscript (2) denotes the 8-bit labels.

The output $\boldsymbol{D}_i^{(2)}$ for $\boldsymbol{A}_i^{(2)}$ is obtained from Eqs. (4)–(6) [14]. Eight labels can be recognized with an infinite contrast ratio for the ideal case of $\alpha_{ij} = 1$.

We now consider the effect of the phase deviation alone by setting $\beta_{ij} = 1$. To find the accumulated effect in the 4-bit basic module and in the connecting waveguides between B_i and C_i, we evaluated the output intensities as a function of ϕ_{12} ($= \phi_{13} = \phi_{32} = \phi_{33}$) as shown in Fig. 5, where the other phases ϕ_{ij} are assumed to be 0. The ratio of $D_{\text{out5}}/D_{\text{out6}}$ is also plotted to evaluate the contrast ratio. For example, the output from D_{out6} increases 5.4 % of the maximum output intensity when the phase deviation is 0.1π rad, where, the contrast ratio decreases to 17.3. Now, we consider the effect of loss in two specific cases. First, we find the effect of β_{12}, β_{13}, β_{32}, and β_{33} on the outputs as a function of L_{12} ($= L_{13} = L_{32} = L_{33}$) as shown in Fig. 6 (a), where other L_{ij} are assumed to be 0. The loss of 2.2 dB in $\beta_{12} = \beta_{13} =$

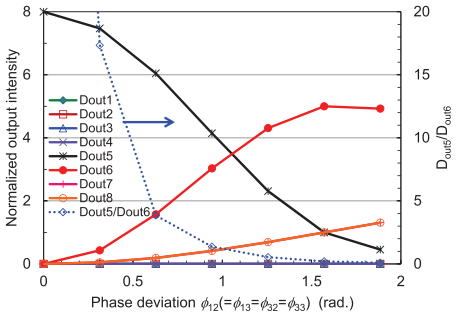

Fig. 5 The output intensities as a function of the phase deviation ϕ_{12} ($= \phi_{13} = \phi_{32} = \phi_{33}$) for the 8-bit recognition circuit, where the other phases ϕ_{ij} are assumed to be 0.

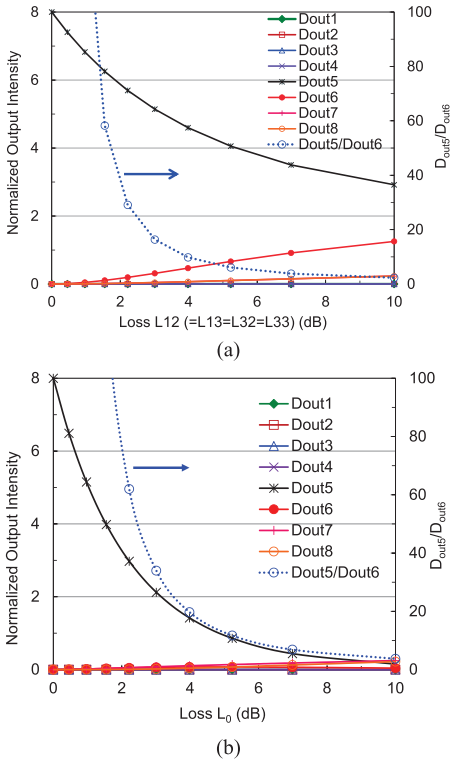

Fig. 6 (a) The output intensities as a function of the waveguide loss L_{12} ($= L_{13} = L_{32} = L_{33}$), where the other losses and the phase deviation are assumed to be 0. (b) The output intensities as a function of L_0, where $L_{11} = L_{14} = L_{21} = L_{24} = L_{31} = L_{38} = 0$ dB, $L_{12} = L_{13} = L_{22} = L_{23} = L_{32} = L_{37} = L_0$, $L_{33} = L_{36} = 2L_0$, and $L_{34} = L_{35} = 3L_0$, and the phase deviation is assumed to be 0.

$\beta_{32} = \beta_{33}$ induces a decrease of 28.8 % and an increase relative to D_{out5} of 2.4 % at D_{out5} and D_{out6}, respectively. The contrast ratio decreases to 29.1. Next, we consider the case where the loss is assumed only at the crossed waveguides. We assume $L_{11} = L_{14} = L_{21} = L_{24} = L_{31} = L_{38} = 0$ dB, $L_{12} = L_{13} = L_{22} = L_{23} = L_{32} = L_{37} = L_0$, $L_{33} = L_{36} = 2L_0$, and $L_{34} = L_{35} = 3L_0$ according to the number of crossed points. The output intensities as a function of L_0 is shown in (b). The loss of 2.2 dB in L_0 induces a decrease of 62.8 % and an increase relative to D_{out5} of 0.6 % at D_{out5} and D_{out6}, respectively. The contrast ratio decreases to 62.0. Although the output intensities decrease due to larger loss through the connecting waveguides, the contrast ratio is larger than the case shown in (a). This is caused by the assumed asymmetric losses in (a).

3. Increase of Recognizable 4-Bit Labels

In this section, we discuss methods to increase the number of recognizable labels by extending the circuits for 4-bit labels.

3.1 Increase by Code Conversion

The basic idea to increase the number of recognizable labels is the extension of the circuit to accept other combination of label codes. Namely, we consider the codes having not only one but also zero or two "−1" components in each label of $\boldsymbol{A}_i$. In order to accept such labels, a code converter circuit Tc is employed in front of the lower 4-bit basic module as shown in Fig. 7 [14]. In the code converter, constant phase shifts

$$\Delta\phi_i = \begin{cases} \pi & (i = 1) \\ 0 & (i = 2, 3, 4) \end{cases} \tag{7}$$

are applied to $A_{\text{in}\,i}$ as $A_{\text{in}\,i}e^{j\Delta\phi_i}$, $i = 1, \ldots, 4$. Using this code converter, four labels $\boldsymbol{A}_5, \boldsymbol{A}_6, \boldsymbol{A}_7, \boldsymbol{A}_8$ defined by

$$(\boldsymbol{A}_5 \;\; \boldsymbol{A}_6 \;\; \boldsymbol{A}_7 \;\; \boldsymbol{A}_8) = \begin{pmatrix} -1 & 1 & -1 & -1 \\ -1 & 1 & 1 & 1 \\ 1 & 1 & 1 & -1 \\ 1 & 1 & -1 & 1 \end{pmatrix} \tag{8}$$

are converted to $\boldsymbol{A}_1, \boldsymbol{A}_2, \boldsymbol{A}_3, \boldsymbol{A}_4$, respectively. Therefore, the outputs $D_{\text{out5}}, \ldots, D_{\text{out8}}$ from the lower 4-bit basic module for $\boldsymbol{A}_5, \boldsymbol{A}_6, \boldsymbol{A}_7$, and $\boldsymbol{A}_8$ are the same as the outputs $D_{\text{out1}}, \ldots, D_{\text{out4}}$ for $\boldsymbol{A}_1, \boldsymbol{A}_2, \boldsymbol{A}_3$, and $\boldsymbol{A}_4$, respectively.

The outputs $(\boldsymbol{D}_1^{(1-1)} \ldots \boldsymbol{D}_4^{(1-1)})$ from the upper 4-bit basic module for $(\boldsymbol{A}_1, \ldots, \boldsymbol{A}_4)$ are given by replacing α_i by α_{1i} in Eq. (3). The outputs $(\boldsymbol{D}_1^{(1-2)} \ldots \boldsymbol{D}_4^{(1-2)})$ from the lower 4-bit basic module are derived as

$$(\boldsymbol{D}_1^{(1-2)} \;\; \boldsymbol{D}_2^{(1-2)} \;\; \boldsymbol{D}_3^{(1-2)} \;\; \boldsymbol{D}_4^{(1-2)}) = \begin{pmatrix} -\alpha_{21} & \alpha_{21} & \alpha_{23} & -\alpha_{23} \\ \alpha_{21} & -\alpha_{21} & \alpha_{23} & -\alpha_{23} \\ -\alpha_{24} & -\alpha_{24} & \alpha_{22} & \alpha_{22} \\ \alpha_{24} & \alpha_{24} & \alpha_{22} & \alpha_{22} \end{pmatrix}. \tag{9}$$

The outputs $(\boldsymbol{D}_5^{(1-1)} \ldots \boldsymbol{D}_8^{(1-1)})$ from the upper 4-bit basic module for $(\boldsymbol{A}_5, \ldots, \boldsymbol{A}_8)$ are derived from Eqs. (1) and (8) as given by replacing α_{2i} by α_{1i} in Eq. (9). The outputs $(\boldsymbol{D}_5^{(1-2)} \ldots \boldsymbol{D}_8^{(1-2)})$ from the lower 4-bit basic module are given by replacing α_i by α_{2i} in Eq. (3).

The ideal output intensities for $\boldsymbol{A}_1, \ldots, \boldsymbol{A}_8$ with $\alpha_{ij} = 1$ are plotted in Fig. 8. The contrast ratio at each output is calculated as $(\pm 2.0)^2/(\pm 1.0)^2 = 4.0$. The decrease of the contrast ratio due to α_{ij} is similar to that in the basic 4-bit module.

3.2 Increase by Sign Identification

Since the number of the 4-bit binary codes is sixteen, only a half of the codes can be recognized in the circuit shown in Fig. 7. The rest codes are complement of $\boldsymbol{A}_i$, $i = 1, \ldots, 8$, that is, $\bar{\boldsymbol{A}}_i$. Although the output fields for $\boldsymbol{A}_i$ and $\bar{\boldsymbol{A}}_i$ are different in the sign, that is, the phase difference of π, they cannot be distinguished by their intensities.

To distinguish the sign of the output field, we introduce interference with a reference pulse $A_{\text{in,r}}$ as shown in Fig. 9. The reference pulse is supposed to have been transmitted together with the label pulse train. The reference pulse $A_{\text{in,r}}$ is amplified with the amplitude amplification coefficient $\sqrt{8}\alpha$, and is divided into eight pulses having amplitude $\alpha A_{\text{in,r}}$. Although, in our previous paper [14], the value of α was assumed to be 1, we try to find an optimum value for α in this paper. The output fields $\boldsymbol{D}^{(1-1)}$ and $\boldsymbol{D}^{(1-2)}$ of the basic modules are interfered with $\alpha A_{\text{in,r}}$ through asymmetric X-junction couplers. For complete interference between the

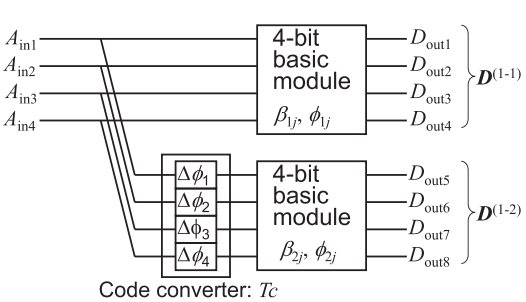

Fig. 7 A circuit to recognize eight 4-bit labels by employing code converter.

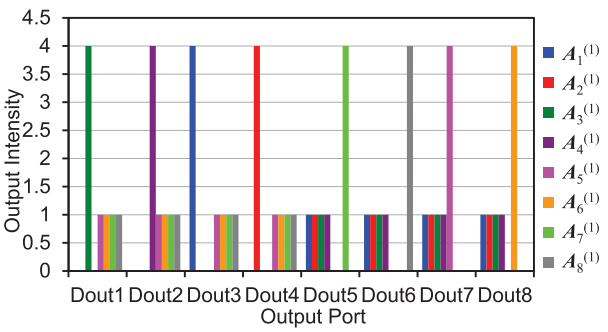

Fig. 8 Ideal output intensities for the eight 4-bit labels $\boldsymbol{A}_1, \ldots, \boldsymbol{A}_8$.

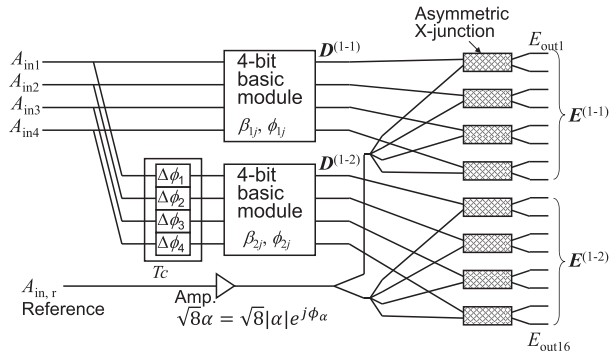

Fig. 9 A circuit to recognize the sixteen 4-bit labels by employing a code converter and interference with a reference pulse.

signals $\boldsymbol{D}^{(1-1)}$, $\boldsymbol{D}^{(1-2)}$, and $\alpha A_{\mathrm{in,r}}$ to distinguish the sign, the phase relation is important. We define $\alpha = |\alpha|e^{j\phi_\alpha}$. The phase ϕ_α corresponds to the phase shift due to the fabrication error or an equivalent phase deviation in the reference signal $A_{\mathrm{in,r}}$. The sixteen output fields $\boldsymbol{E}^{(1-1)}$ and $\boldsymbol{E}^{(1-2)}$ are related to the output fields $\boldsymbol{D}^{(1-1)}$ and $\boldsymbol{D}^{(1-2)}$, and the reference $\alpha A_{\mathrm{in,r}}$ as

$$\begin{aligned}\boldsymbol{E}^{(1-1)} &= (E_{\mathrm{out1}}, \ldots, E_{\mathrm{out8}})^t \\ &= Tx_4(D_{\mathrm{out1}}, \ldots, D_{\mathrm{out4}}, \alpha A_{\mathrm{in,r}})^t,\end{aligned} \tag{10}$$

and

$$\begin{aligned}\boldsymbol{E}^{(1-2)} &= (E_{\mathrm{out9}}, \ldots, E_{\mathrm{out16}})^t \\ &= Tx_4(D_{\mathrm{out5}}, \ldots, D_{\mathrm{out8}}, \alpha A_{\mathrm{in,r}})^t,\end{aligned} \tag{11}$$

where

$$Tx_4 = \frac{1}{\sqrt{2}}\begin{pmatrix} 1 & 0 & 0 & 0 & 1 \\ -1 & 0 & 0 & 0 & 1 \\ 0 & 1 & 0 & 0 & 1 \\ 0 & -1 & 0 & 0 & 1 \\ 0 & 0 & 1 & 0 & 1 \\ 0 & 0 & -1 & 0 & 1 \\ 0 & 0 & 0 & 1 & 1 \\ 0 & 0 & 0 & -1 & 1 \end{pmatrix}. \tag{12}$$

We assume $A_{\mathrm{in,r}} = 1$. The output fields $\boldsymbol{E}^{(1-1)}$ and $\boldsymbol{E}^{(1-2)}$ for $(\boldsymbol{A}_1 \ldots \boldsymbol{A}_4)$ are given by

$$\begin{aligned}&(\boldsymbol{E}_1^{(1-1)} \ \boldsymbol{E}_2^{(1-1)} \ \boldsymbol{E}_3^{(1-1)} \ \boldsymbol{E}_4^{(1-1)}) \\ &= Tx_4\begin{pmatrix} \boldsymbol{D}_1^{(1-1)} & \boldsymbol{D}_2^{(1-1)} & \boldsymbol{D}_3^{(1-1)} & \boldsymbol{D}_4^{(1-1)} \\ \alpha & \alpha & \alpha & \alpha \end{pmatrix},\end{aligned} \tag{13}$$

where $\boldsymbol{D}_j^{(1-1)}$ are given by replacing α_i by α_{1i} in Eq. (3).

$$\begin{aligned}&(\boldsymbol{E}_1^{(1-2)} \ \boldsymbol{E}_2^{(1-2)} \ \boldsymbol{E}_3^{(1-2)} \ \boldsymbol{E}_4^{(1-2)}) \\ &= Tx_4\begin{pmatrix} \boldsymbol{D}_1^{(1-2)} & \boldsymbol{D}_2^{(1-2)} & \boldsymbol{D}_3^{(1-2)} & \boldsymbol{D}_4^{(1-2)} \\ \alpha & \alpha & \alpha & \alpha \end{pmatrix},\end{aligned} \tag{14}$$

where $\boldsymbol{D}_i^{(1-2)}$ are given by Eq. (9).

For $(\boldsymbol{A}_5 \ldots \boldsymbol{A}_8)$, $(\boldsymbol{E}_5^{(1-1)} \ldots \boldsymbol{E}_8^{(1-1)})$ and $(\boldsymbol{E}_5^{(1-2)} \ldots \boldsymbol{E}_8^{(1-2)})$ are obtained from Eq. (14) with the replacement of α_{2i} by α_{1i} and Eq. (13) with the replacement of α_{1i} by α_{2i}, respectively.

We define $\boldsymbol{A}_9, \boldsymbol{A}_{10}, \boldsymbol{A}_{11}, \boldsymbol{A}_{12}$ as $\bar{\boldsymbol{A}}_1, \bar{\boldsymbol{A}}_2, \bar{\boldsymbol{A}}_3, \bar{\boldsymbol{A}}_4$, respectively. For these labels, the output fields $(\boldsymbol{E}_9^{(1-1)} \ldots \boldsymbol{E}_{12}^{(1-1)})$ and $(\boldsymbol{E}_9^{(1-2)} \ldots \boldsymbol{E}_{12}^{(1-2)})$ are given by replacing α_{ji} by $-\alpha_{ji}$ in Eqs. (13) and (14), respectively.

We also define $\boldsymbol{A}_{13}, \boldsymbol{A}_{14}, \boldsymbol{A}_{15}, \boldsymbol{A}_{16}$ as $\bar{\boldsymbol{A}}_5, \bar{\boldsymbol{A}}_6, \bar{\boldsymbol{A}}_7, \bar{\boldsymbol{A}}_8$, respectively. For these labels, $(\boldsymbol{E}_{13}^{(1-1)} \ldots \boldsymbol{E}_{16}^{(1-1)})$ and

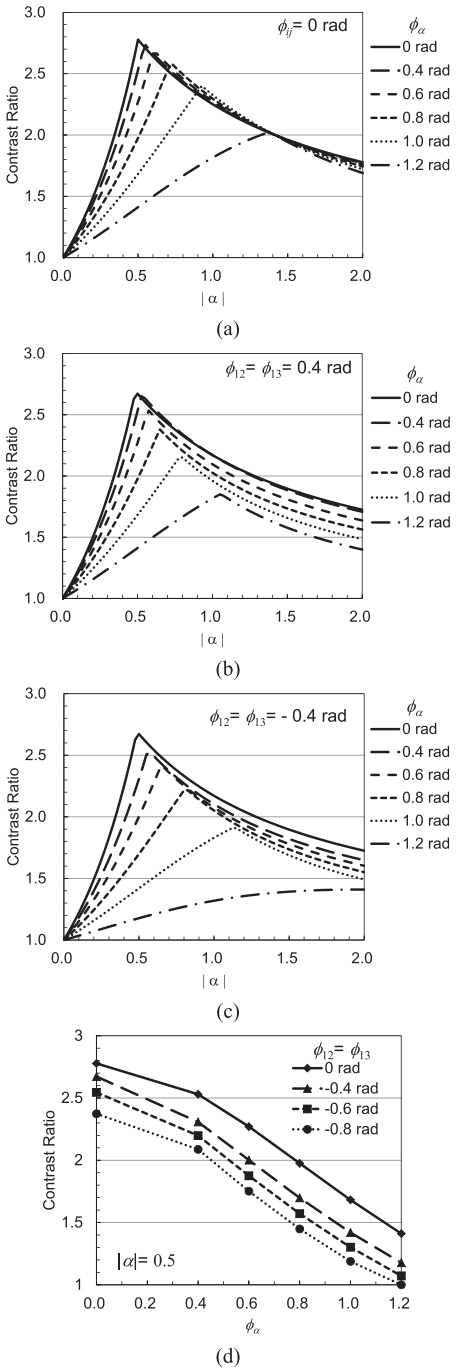

Fig. 10 The contrast ratio as a function of $|\alpha|$ for the sixteen 4-bit labels for the phases ϕ_{ij} of α_{ij} are 0 in (a), for $\phi_{12} = \phi_{13} = 0.4$ rad. and other $\phi_{ij} = 0$ in (b), and for $\phi_{12} = \phi_{13} = -0.4$ rad. and other $\phi_{ij} = 0$ in (c). The contrast ratio at $|\alpha| = 0.5$ as a function of ϕ_α is summarized in (d).

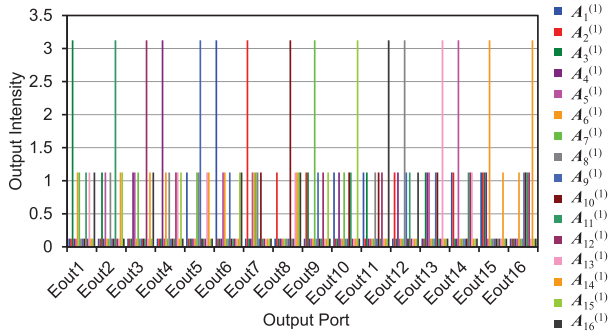

Fig. 11 Ideal output intensities at $\alpha = 0.5$ for the sixteen 4-bit labels.

$(\boldsymbol{E}_{13}^{(1-2)} \dots \boldsymbol{E}_{16}^{(1-2)})$ are given by replacing α_{2i} by $-\alpha_{1i}$ in Eq. (14) and by replacing α_{1i} by $-\alpha_{2i}$ in Eq. (13), respectively.

The contrast ratio of the output intensities depends on the value α as shown in Fig. 10, where the phase ϕ_α of α is varied as a parameter. Three typical cases are shown for the phases ϕ_{ij} of α_{ij} are 0 in (a), for $\phi_{12} = \phi_{13} = 0.4$ rad. and other $\phi_{ij} = 0$ in (b), and for $\phi_{12} = \phi_{13} = -0.4$ rad. and other $\phi_{ij} = 0$ in (c). The contrast ratio at $|\alpha| = 0.5$ as a function of ϕ_α is summarized in (d), where ϕ_{ij} is varied from 0 to -0.8 rad. The sign of ϕ_{ij} is assumed to be different from that of ϕ_α to evaluate the worst phase-error combinations. If the requited contrast ratio for the label recognition is 1.5, it is roughly estimated that the phase error of ϕ_{ij} and ϕ_α has to be less than around 0.8 rad.

For the ideal case of $\phi_\alpha = \phi_{ij} = 0$, the maximum output intensity is $[(2 + \alpha)/\sqrt{2}]^2$. The second largest output intensity is the larger value between $[(-2 + \alpha)/\sqrt{2}]^2$ and $[(1 + \alpha)/\sqrt{2}]^2$. Therefore, the maximum contrast ratio of $[(2+\alpha)/\sqrt{2}]^2/Max([(-2+\alpha)/\sqrt{2}]^2, [(1+\alpha)/\sqrt{2}]^2) = 2.78$ is obtained when $[(-2 + \alpha)/\sqrt{2}]^2 = [(1 + \alpha)/\sqrt{2}]^2$, that is, $\alpha = 0.5$. The output intensities at $\alpha = 0.5$ for all sixteen labels are plotted in Fig. 11.

4. Increase of Recognizable 8-Bit Labels

4.1 Increase by Code Conversion

In similar manner as the 4-bit label recognition, we consider a recognition circuit for a half of the 8-bit binary codes as shown in Fig. 12. The 8-bit basic module is the circuit shown in Fig. 4. A code converter Tc_k is placed in front of the kth 8-bit basic module, where $k = 1, \dots, 16$. Each code converter consists of parallel eight phase shifters with the phase shift amount of $\Delta\phi_i, i = 1, \dots, 8$ as follows:

- For $Tc_k, k = 1$; $\Delta\phi_i = 0$ $(i = 1, \dots, 8)$
- For $Tc_k, k = 2, \dots, 9$; $\Delta\phi_{k-1} = \pi$ and $\Delta\phi_i = 0$ $(i \neq k - 1)$
- For $Tc_k, k = 10, \dots, 16$; $\Delta\phi_1 = \pi$, $\Delta\phi_{k-8} = \pi$ and $\Delta\phi_i = 0$ $(i \neq 1$ or $i \neq k - 8)$.

Only one and two components of an incident code are inverted with $Tc_k, k = 2, \dots, 9$, and $Tc_k, k = 10, \dots, 16$, respectively. Using these converters and the 8-bit basic modules, the 128 optical labels shown in Table 1 can be recognized. The decimal number for each label calculated by $(A_{\text{in1}} + 1)/2 + (A_{\text{in2}} + 1)2^1/2 + \cdots + (A_{\text{in8}} + 1)2^7/2$ is also given in this table to show that these labels are nonidentical with each other.

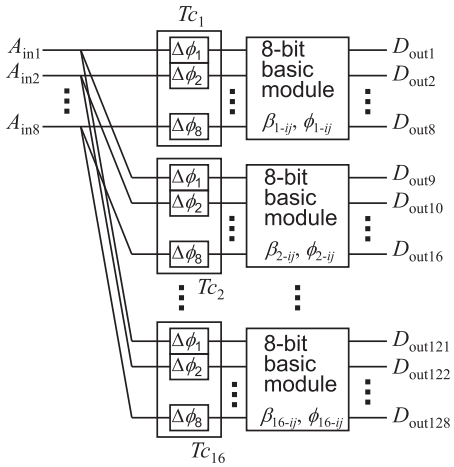

Fig. 12 A circuit to recognize the 128 8-bit labels by employing code converters.

The output intensities for these labels are calculated by using Eqs. (4) and (5). Some typical parts of the ideal output intensities for labels $(\boldsymbol{A}_1^{(2)} \dots \boldsymbol{A}_8^{(2)})$, $(\boldsymbol{A}_9^{(2)} \dots \boldsymbol{A}_{16}^{(2)})$, and $(\boldsymbol{A}_{73}^{(2)} \dots \boldsymbol{A}_{80}^{(2)})$ are plotted in Fig. 13 (a), (b), and (c), respectively, where α_{k-ij} are assumed to be 1. The contrast ratio for these 128 label recognition is $[8/(2\sqrt{2})/(6/(2\sqrt{2}))]^2 = 1.78$. If the system is separated into two groups, that is, $(Tc_1, Tc_{10}, \dots, Tc_{16})$ and $(Tc_2, \dots, Tc_9)$, the contrast ratio for each group is $[8/(2\sqrt{2})/(4/(2\sqrt{2}))]^2 = 4.0$, where 64 labels are recognized in each system.

4.2 Increase by Sign Identification

To recognize all the 8-bit binary labels, we introduce interference with a reference pulse as shown in Fig. 14, where the kth code converter and the 8-bit basic module are illustrated. Since sixteen similar circuits for $k = 1, \dots, 16$ are connected in parallel, the incident signals $A_{\text{in1}}, \dots, A_{\text{in8}}$, and $A_{\text{in,r}}$ are divided into sixteen signals. However, for simplicity, the signals of amplitudes $A_{\text{in1}}, \dots, A_{\text{in8}}$, and $A_{\text{in,r}}$ are assumed to be input into each parallel circuits.

The output fields $E_{\text{out16}(k-1)+m}, m, k = 1, \dots, 16$, are related to the output fields of 8-bit basic modules $D_{\text{out}(k-1)+m}, m = 1, \dots, 8$, and the reference signal $A_{\text{in,r}}$ as

$$\begin{pmatrix} E_{\text{out16}(k-1)+1} \\ E_{\text{out16}(k-1)+2} \\ \vdots \\ E_{\text{out16}(k-1)+16} \end{pmatrix} = Tx_8 \begin{pmatrix} D_{\text{out}(k-1)+1} \\ \vdots \\ D_{\text{out}(k-1)+8} \\ A_{\text{in,r}} \end{pmatrix}, \tag{15}$$

where

Table 1 Recognizable 128 8-bit label by code conversion.

Tc_1:	$(A_1^{(2)} \dots A_8^{(2)})$	$= \begin{pmatrix} A_1A_1A_2A_2A_3A_3A_4A_4 \\ A_1\bar{A}_1A_2\bar{A}_2A_3\bar{A}_3A_4\bar{A}_4 \end{pmatrix}$ $\rightarrow$ (221 45 238 30 119 135 187 75)
Tc_2:	$(A_9^{(2)} \dots A_{16}^{(2)})$	$= \begin{pmatrix} A_5A_5A_6A_6A_7A_7A_8A_8 \\ A_1\bar{A}_1A_2\bar{A}_2A_3\bar{A}_3A_4\bar{A}_4 \end{pmatrix}$ $\rightarrow$ (220 44 239 31 118 134 186 74)
Tc_3:	$(A_{17}^{(2)} \dots A_{24}^{(2)})$	$= \begin{pmatrix} A_6A_6A_5A_5\bar{A}_8\bar{A}_8\bar{A}_7\bar{A}_7 \\ A_1\bar{A}_1A_2\bar{A}_2A_3\bar{A}_3A_4\bar{A}_4 \end{pmatrix}$ $\rightarrow$ (223 47 236 28 117 133 185 73)
Tc_4:	$(A_{25}^{(2)} \dots A_{32}^{(2)})$	$= \begin{pmatrix} \bar{A}_7\bar{A}_7A_8A_8\bar{A}_5\bar{A}_5A_6A_6 \\ A_1\bar{A}_1A_2\bar{A}_2A_3\bar{A}_3A_4\bar{A}_4 \end{pmatrix}$ $\rightarrow$ (217 41 234 26 115 131 191 79)
Tc_5:	$(A_{33}^{(2)} \dots A_{40}^{(2)})$	$= \begin{pmatrix} \bar{A}_8\bar{A}_8A_7A_7A_6A_6\bar{A}_5\bar{A}_5 \\ A_1\bar{A}_1A_2\bar{A}_2A_3\bar{A}_3A_4\bar{A}_4 \end{pmatrix}$ $\rightarrow$ (213 37 230 22 127 143 179 67)
Tc_6:	$(A_{41}^{(2)} \dots A_{48}^{(2)})$	$= \begin{pmatrix} A_1A_1A_2A_2A_3A_3A_4A_4 \\ A_5\bar{A}_5A_6\bar{A}_6A_7\bar{A}_7A_8\bar{A}_8 \end{pmatrix}$ $\rightarrow$ (205 61 254 14 103 151 171 91)
Tc_7:	$(A_{49}^{(2)} \dots A_{56}^{(2)})$	$= \begin{pmatrix} A_1A_1A_2A_2A_3A_3A_4A_4 \\ A_6\bar{A}_6A_5\bar{A}_5\bar{A}_8A_8\bar{A}_7A_7 \end{pmatrix}$ $\rightarrow$ (253 13 206 62 87 167 155 107)
Tc_8:	$(A_{57}^{(2)} \dots A_{64}^{(2)})$	$= \begin{pmatrix} A_1A_1A_2A_2A_3A_3A_4A_4 \\ \bar{A}_7A_7A_8\bar{A}_8\bar{A}_5A_5A_6\bar{A}_6 \end{pmatrix}$ $\rightarrow$ (157 109 174 94 55 199 251 11)
Tc_9:	$(A_{65}^{(2)} \dots A_{72}^{(2)})$	$= \begin{pmatrix} A_1A_1A_2A_2A_3A_3A_4A_4 \\ \bar{A}_8A_8A_7\bar{A}_7A_6\bar{A}_6\bar{A}_5A_5 \end{pmatrix}$ $\rightarrow$ (93 173 110 158 247 7 59 203)
Tc_{10}:	$(A_{73}^{(2)} \dots A_{80}^{(2)})$	$= \begin{pmatrix} A_2A_2A_1A_1\bar{A}_4\bar{A}_4\bar{A}_3\bar{A}_3 \\ A_1\bar{A}_1A_2\bar{A}_2A_3\bar{A}_3A_4\bar{A}_4 \end{pmatrix}$ $\rightarrow$ (222 46 237 29 116 132 184 72)
Tc_{11}:	$(A_{81}^{(2)} \dots A_{88}^{(2)})$	$= \begin{pmatrix} \bar{A}_3\bar{A}_3A_4A_4\bar{A}_1\bar{A}_1A_2A_2 \\ A_1\bar{A}_1A_2\bar{A}_2A_3\bar{A}_3A_4\bar{A}_4 \end{pmatrix}$ $\rightarrow$ (216 40 235 27 114 130 190 78)
Tc_{12}:	$(A_{89}^{(2)} \dots A_{96}^{(2)})$	$= \begin{pmatrix} \bar{A}_4\bar{A}_4A_3A_3A_2A_2\bar{A}_1\bar{A}_1 \\ A_1\bar{A}_1A_2\bar{A}_2A_3\bar{A}_3A_4\bar{A}_4 \end{pmatrix}$ $\rightarrow$ (212 36 231 23 126 142 178 66)
Tc_{13}:	$(A_{97}^{(2)} \dots A_{104}^{(2)})$	$= \begin{pmatrix} A_5A_5A_6A_6A_7A_7A_8A_8 \\ A_5\bar{A}_5A_6\bar{A}_6A_7\bar{A}_7A_8\bar{A}_8 \end{pmatrix}$ $\rightarrow$ (204 60 255 15 102 150 170 90)
Tc_{14}:	$(A_{105}^{(2)} \dots A_{112}^{(2)})$	$= \begin{pmatrix} A_5A_5A_6A_6A_7A_7A_8A_8 \\ A_6\bar{A}_6A_5\bar{A}_5\bar{A}_8A_8\bar{A}_7A_7 \end{pmatrix}$ $\rightarrow$ (252 12 207 63 86 166 154 106)
Tc_{15}:	$(A_{113}^{(2)} \dots A_{120}^{(2)})$	$= \begin{pmatrix} A_5A_5A_6A_6A_7A_7A_8A_8 \\ \bar{A}_7A_7A_8\bar{A}_8\bar{A}_5A_5A_6\bar{A}_6 \end{pmatrix}$ $\rightarrow$ (156 108 175 95 54 198 250 10)
Tc_{16}:	$(A_{121}^{(2)} \dots A_{128}^{(2)})$	$= \begin{pmatrix} A_5A_5A_6A_6A_7A_7A_8A_8 \\ \bar{A}_8A_8A_7\bar{A}_7A_6\bar{A}_6\bar{A}_5A_5 \end{pmatrix}$ $\rightarrow$ (92 172 111 159 246 6 58 202)

$$Tx_8 = \frac{1}{\sqrt{2}} \begin{pmatrix} 1 & 0 & 0 & 0 & 0 & 0 & 0 & 0 & 1 \\ -1 & 0 & 0 & 0 & 0 & 0 & 0 & 0 & 1 \\ 0 & 1 & 0 & 0 & 0 & 0 & 0 & 0 & 1 \\ 0 & -1 & 0 & 0 & 0 & 0 & 0 & 0 & 1 \\ 0 & 0 & 1 & 0 & 0 & 0 & 0 & 0 & 1 \\ 0 & 0 & -1 & 0 & 0 & 0 & 0 & 0 & 1 \\ 0 & 0 & 0 & 1 & 0 & 0 & 0 & 0 & 1 \\ 0 & 0 & 0 & -1 & 0 & 0 & 0 & 0 & 1 \\ 0 & 0 & 0 & 0 & 1 & 0 & 0 & 0 & 1 \\ 0 & 0 & 0 & 0 & -1 & 0 & 0 & 0 & 1 \\ 0 & 0 & 0 & 0 & 0 & 1 & 0 & 0 & 1 \\ 0 & 0 & 0 & 0 & 0 & -1 & 0 & 0 & 1 \\ 0 & 0 & 0 & 0 & 0 & 0 & 1 & 0 & 1 \\ 0 & 0 & 0 & 0 & 0 & 0 & -1 & 0 & 1 \\ 0 & 0 & 0 & 0 & 0 & 0 & 0 & 1 & 1 \\ 0 & 0 & 0 & 0 & 0 & 0 & 0 & -1 & 1 \end{pmatrix}. \quad (16)$$

First, we consider an ideal case of $\alpha_{k-ij} = 1$ and $\phi_\alpha = 0$.

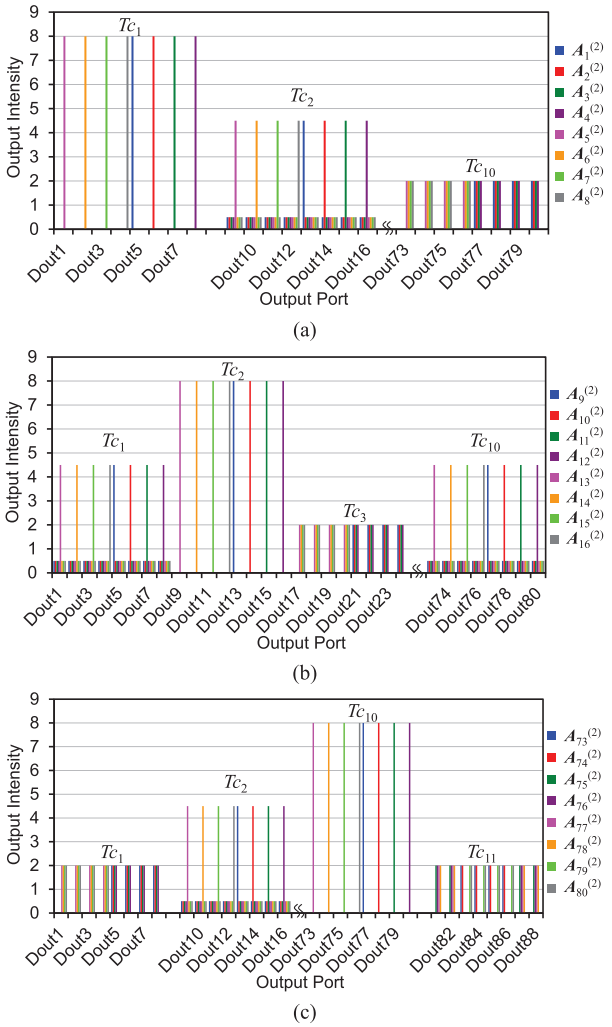

Fig. 13 The output intensities at the partial output ports for the 128 8-bit labels with the circuits having code converters for (a) $(A_1^{(2)}, \dots, A_8^{(2)})$, (b) $(A_9^{(2)}, \dots, A_{16}^{(2)})$, and (c) $(A_{73}^{(2)}, \dots, A_{80}^{(2)})$.

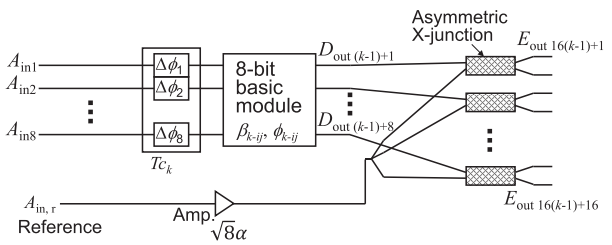

Fig. 14 A circuit to recognize the 256 8-bit labels by employing a code converter and interference with a reference pulse, where the kth partial circuit is illustrated.

The maximum output E_{outk} is $(2\sqrt{2}+\alpha)/\sqrt{2}$. The minimum value of the secondly largest output is $|(-2\sqrt{2}+\alpha)/\sqrt{2}| = |(6+2\sqrt{2}\alpha)/4|$ when $\alpha = \sqrt{2}/4 \simeq 0.354$. The maximum contrast ratio is found to be $[((2\sqrt{2}+\alpha)/\sqrt{2})/((-2\sqrt{2}+\alpha)/\sqrt{2})]^2 \simeq 1.653$ at $\alpha \simeq 0.354$. The output intensities of $E_{out1}, \dots, E_{out32}, E_{out145}, \dots, E_{out160}$ are plotted for labels $A_1^{(2)}, \dots, A_8^{(2)}$ in Fig. 15. These characteristics are the same for the other labels. Thus, all binary 8-bit labels

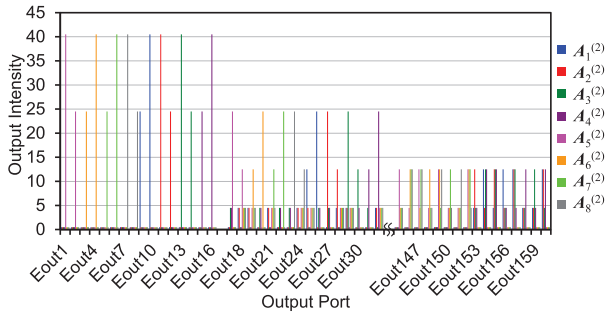

Fig. 15 The output intensities of $E_{\text{out1}}, \ldots, E_{\text{out32}}, E_{\text{out145}}, \ldots, E_{\text{out160}}$ at $\alpha = 0.354$ for the eight 8-bit labels $\boldsymbol{A}_1^{(2)}, \ldots, \boldsymbol{A}_8^{(2)}$.

can be recognized with a contrast ratio of 1.653. If the labels are divided into two groups, namely, the labels for $(Tc_1, Tc_{10}, \ldots, Tc_{16})$ and for $(Tc_2, \ldots, Tc_9)$, the minimum value of the second highest output can be $|(-2\sqrt{2}+\alpha)/\sqrt{2}| = |(4 + 2\sqrt{2}\alpha)/4|$ when $\alpha = 1/\sqrt{2} \simeq 0.707$. With this α, the contrast ratio becomes $[((2\sqrt{2} + \alpha)/\sqrt{2})/((-2\sqrt{2} + \alpha)/\sqrt{2})]^2 \simeq 2.778$.

Next, we consider the effect of phases ϕ_α and ϕ_{k-ij}. The minimum contrast ratio for the 128 and 256 labels is plotted as a function of $|\alpha|$ in Fig. 16 for the cases of $\phi_{k-i2} = \phi_{k-i3} = 0$, 0.4, and -0.4 rad. in (a), (b), and (c), respectively, where ϕ_α is varied as a parameter. The contrast ratio at $|\alpha| = 0.7$ and 0.35 for 128 and 256 labels, respectively, as a function of ϕ_α is summarized in (d). It is found that the contrast ratio decreases due to the phase deviation of ϕ_α and ϕ_{k-ij} for a constant $|\alpha|$. If the constant ratio required for the label recognition is supposed to be 1.5, it is roughly estimated that the phase error of ϕ_{k-ij} and ϕ_α has to be less than around 0.5 and 0.4 rad for 128 and 256 labels, respectively.

5. Discussion

The proposed circuits for the 4-bit BPSK labels can recognize 4, 8, and 16 labels with a contrast ratio of infinity, 4.00, and 2.78, respectively for the ideal cases of no phase shift. The circuits for the 8-bit labels can recognize 8, 64, 128, and 256 labels with a contrast ratio of infinity, 4.00, 2.78, and 1.65, respectively for the cases of no phase shift.

We compare these results with the tree-structure waveguide circuits with asymmetric X-junction couplers reported by Hiura *et al.* [12] designed for 2^N N-bit BPSK labels. The number of recognizable bits can be increased with the number of concatenating stage of the asymmetric X-junction couplers. Four, eight, and sixteen labels corresponding to 2-, 3-, and 4-bit BPSK labels can be recognized with a contrast ratio of 9.00, 4.00, and 2.78, respectively. Similarly, 64, 128, and 256 labels corresponding to 6-, 7-, and 8-bit BPSK labels can be recognized with a contrast ratio of 1.96, 1.78, and 1.65, respectively. These contrast ratios for 64, 128, and 256 labels are plotted in Fig. 17 compared with the circuits proposed in this paper. It is found that contrast ratios of this work are larger than or equal to that of the tree-structured circuits. Therefore, the circuits proposed in this

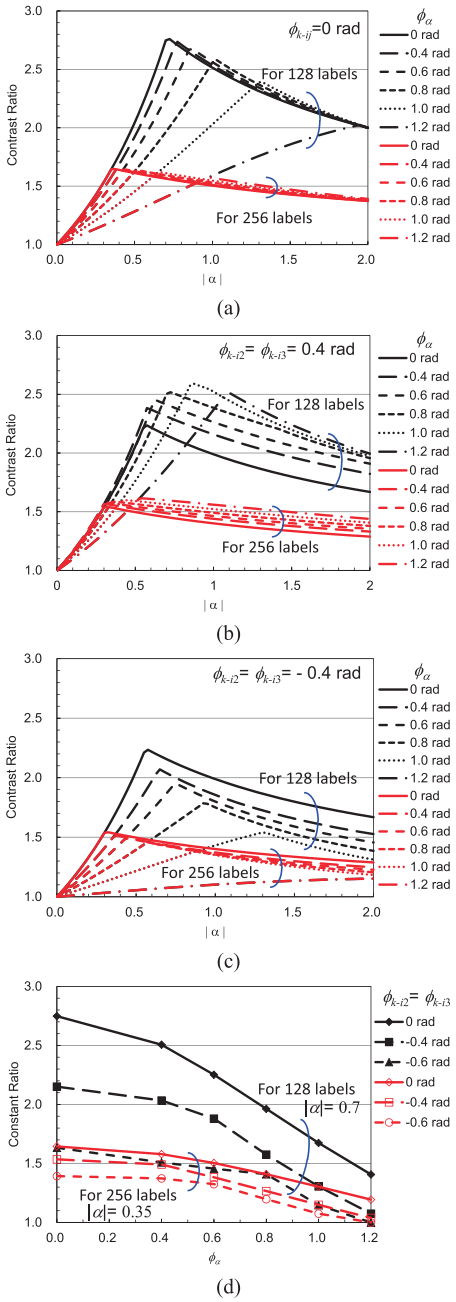

Fig. 16 The contrast ratio as a function of α for the 256 and the classified 128 8-bit labels for the cases of (a) $\phi_{k-ij} = 0$, (b) $\phi_{k-ij} = 0.4$ rad., and (c) $\phi_{k-ij} = -0.4$ rad. The contrast ratio at $|\alpha| = 0.7$ and 0.35 for the 128 and 256 labels, respectively, as a function of ϕ_α is summarized in (d).

paper can relax the requirement such as a dynamic range of post-processing thresholding devices. When the recognizable label number is maximized, both circuits show the same contrast ratio because they only consist of passive elements.

We consider the influence of the incident optical intensity on the recognition performance. When the number of labels increase, the incident intensities to the optical circuits, e.g. 8-bit basic modules in Fig. 12, decrease due to power dividers for parallel processing. Since the optical cir-

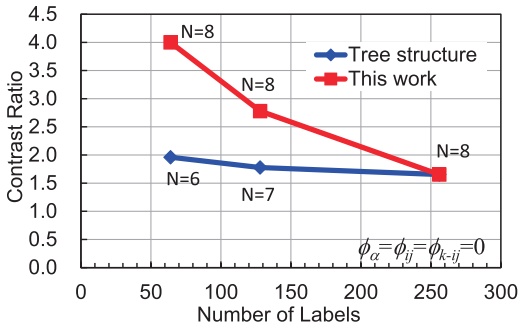

Fig. 17 The contrast ratio as a function of the number of recognizable labels with the tree-structure circuit proposed by Hiura *et al.* and the circuit of this work, where N is the number of bits.

cuits consist of passive waveguides and passive waveguide components, the S/N of the optical signal is expected to degrade only due to scattering and crosstalk in the waveguide components and does not depend on the incident power. However, when the output optical intensities decrease, the detected electric signals degrade due to additive noise at detectors and electronic amplifiers. Similar degradation is expected when the optical label intensities incident at the recognition circuits decrease.

Finally, we consider the scalability of the proposed circuits. It was reported that 32-bit labels were employed in the burst optical packet switching [15]. Since the 8-bit basic module consists of the two 4-bit basic modules, a 16-bit basic module can be composed with the two 8-bit basic modules. However, as shown in Fig. 17, the contrast ratio decreases with the employed number of labels. Therefore, from the viewpoint of the contrast ratio, the employed number of labels has to be limited for a given bit number. To increase further the number of labels without sacrificing the contrast ratio, a multi-stage recognition process can be considered. For instance, if the incident 32-bit labels are demultiplexed into four time-series of 8-bit labels prior to the recognition, the 8-bit basic module can be applied for each time slot. In this case, additional memory and post-processing functions with the help of electronic processing would be required to recognize all of the labels.

6. Conclusion

The optical passive waveguide circuits for the recognition of BPSK labels have been discussed. The proposed circuits can recognize eight and sixteen labels of the 4-bit BPSK labels with a contrast ratio of 4.00 and 2.78, respectively. The 8-bit BSPK labels, 64, 128, and 256 labels can be recognized with a contrast ratio of 4.00, 2.78, and 1.65, respectively. The number of recognizable labels can be increased to all binary encoded labels at the expense of reduction of the contrast ratio.

The decrease of the contrast ratio due to the phase deviation and the propagation loss through optical waveguides was also investigated. Although the effect of phase error is large, it can be reduced by introducing a phase adjusting mechanism in the waveguide devices. Optical path-length adjusting waveguides as introduced in [14] are considered to be useful to simplify the phase adjustment. A systematic procedure for the phase adjustment for all the labels may be required when the number of labels increases.

Since the circuits consist of passive waveguide components, various materials such as silica glass and silicon can be employed.

Acknowledgments

This work was supported in part by JSPS KAKENHI (15H06443).

References

[1] D.J. Blumenthal, B.-E. Olsson, G. Rossi, T.E. Dimmich, L. Rau, M. Masanovic, O. Lavrova, R. Doshi, O. Jerphagnon, J.E. Bowers, V. Kaman, L.A. Coldren, and J. Barton, "All-optical label swapping networks and technologies," J. Lightw. Technol., vol.18, no.12, pp.2058–2075, Dec. 2000.

[2] K. Kitayama, N. Wada, and H. Sotobayashi, "Architectural considerations for photonic IP router based upon optical code correlation," J. Lightw. Technol., vol.18, no.12, pp.1834–1844, Dec. 2000.

[3] M. Aljada and K. Alameh, "Passive and active optical bit-pattern recognition structures for multiwavelength optical packet switching networks," Optics Express, vol.15, no.11. pp.6914–6925, May 2007.

[4] H. Furukawa, T. Konishi, K. Itoh, N. Wada, and T. Miyazaki, "Discrimination of all types of 4-bit optical code by optical time-gating and designed label recognition filter in label recognition using optical correlation," IEICE Trans. Commun., vol.E88-B, no.10, pp.3841–3847, Oct. 2005.

[5] N. Kawakami, K. Shimizu, N. Wada, F. Kubota, and K. Kodate, "All-optical holographic label processing for photonic packet switching," Optical Review, vol.11, no.2, pp.126–131, Feb. 2004.

[6] H. Tsunematsu, T. Arima, N. Goto, and S.-I. Yanagiya, "Photonic label recognition by time-space conversion and two-dimensional spatial filtering with delay compensation," J. Lightw. Technol., vol.27. no.14, pp.2698–2706, July 2009.

[7] F. Moritsuka, N. Wada, T. Sakamoto, T. Kawanishi, Y. Komai, S. Anzai, M. Izutsu, and K. Kodate, "Multiple optical code-label processing using multi-wavelength frequency comb generator and multi-port optical spectrum synthesizer," Optics Express, vol.15, no.12, pp.7515–7521, June 2007.

[8] G. Manzacca, M.S. Moreolo, and G. Cincotti, "Performance analysis of multidimensional codes generated/processed by a single planar devices," J. Lightw. Technol., vol.25, no.6, pp.1629–1637, June 2007.

[9] O. Moriwaki, T. Kitoh, T. Sakamoto, and A. Okada, "Novel PLC-based optical correlator for multiple phase-modulated labels," IEEE Photon. Technol. Lett., vol.17, no.2, pp.489–491, Feb. 2005.

[10] G. Cincotti, "Full optical encoders/decoders for photonic IP routers," J. Lightw. Technol., vol.22, no.2, pp.337–342, Feb. 2004.

[11] H. Hiura, J. Narita, and N. Goto, "Optical label recognition using tree-structure self-routing circuits consisting of asymmetric X-junctions," IEICE Trans. Electron., vol.E90-C, no.12, pp.2270–2277, Dec. 2007.

[12] H. Hiura, N. Goto, and S.-I. Yanagiya, "Wavelength-insensitive integrated-optic circuit consisting of asymmetric X-junction couplers for recognition of BPSK labels," J. Lightw. Technol., vol.27, no.24, pp.5543–5551, Dec. 2009.

[13] M. Izutsu, A. Enokikara, and T. Sueta, "Optical-waveguide hybrid coupler," Optics Letters, vol.7, no.11, pp.549–551, Nov. 1982.

[14] A. Ihara, H. Kishikawa, N. Goto, and S.-I. Yanagiya, "Passive waveguide device consisting of cascaded asymmetric X-junction couplers

for high-contrast recognition of optical BPSK labels," J. Lightw. Technol., vol.29, no.9, pp.1306–1313, May 2011.
[15] T. Segawa, S. Ibrahim, T. Nakahara, Y. Muranaka, and R. Takahashi, "Low-power optical packet switching for 10-Gb/s burst optical packets with a label processor and 8×8 optical switch," J. Lightw. Technol., vol.34, no.8, pp.1844–1850, April 2016.

Hiroki Kishikawa received the B.E. and M.E. degree in information and computer sciences from Toyohashi University of Technology, Toyohashi, Japan in 2004 and 2006, respectively, and the D.E. degree in optical science and technology from Tokushima University, Japan, in 2012. He worked for Nomura Research Institute from 2006 to 2009. He was Research Fellow of Japan Society for the Promotion of Science from 2010 to 2012. From August 2010 to January 2011, he was with McGill University, Montreal, QC, Canada, as a graduate research trainee, where he engaged in research on optical packet format conversion. From April 2012 to March 2015, he worked for Network Innovation Laboratories, NTT Corporation. Since April 2015, he has been an Assistant Professor with Tokushima University. His research interests include photonic routing, photonic switching, and photonic networking. Dr. Kishikawa received the Yasujiro Niwa Outstanding Paper Award in 2011 and the Young Engineer Award of the IEICE of Japan in 2013.

Akito Ihara received the B.E. and M.E. degrees in optical science and technology from Tokushima University, Japan, in 2010 and 2012, respectively. He is presently with Fujitsu Systems West Ltd. His research interests include photonic routing and photonic networking.

Nobuo Goto received the B.E., M.E., and D.E. degrees in electrical and electronics engineering from Nagoya University, Nagoya, Japan, in 1979, 1981, and 1984, respectively. From 1984 to 1986, he was a Research Associate with the Faculty of Engineering, Nagoya University. He became a Research Associate, a Lecturer, and an Associate Professor at Toyohashi University of Technology, Toyohashi, Japan, in 1986, 1989, and 1993 respectively. From August 1987 to August 1988, he was with McGill University, Montreal, QC, Canada, where he was engaged in research on passive and electrooptic integrated devices. From August 2001 to August 2002, he was with the Multimedia University, Malaysia, as Japan International Cooperation Agency (JICA) expert for JICA project of networked multimedia education system. Since April 2007, he has been a Professor with Tokushima University, Tokushima, Japan. His current research interest includes integrated optical signal processing using acoustooptic effects and photonic routing systems. Dr. Goto received the Young Engineer Award of the IEICE of Japan in 1984 and the Niwa Memorial Prize in 1985. He is also a member of IEE of Japan and IEEE.

Shin-ichiro Yanagiya received the B.E. and M.E. degrees in physics from Tohoku University, Japan in 1996 and 1998, respectively and D.E. degree in optical science and technology from Tokushima University, Japan, in 2005. He is an Assistant Professor in the Department of Optical Science and Technology, Tokushima University, Japan. He was a visiting researcher in The Edward S. Rogers, Sr. Department of Electrical and Computer Engineering, University of Toronto from September 2008 to February 2009. His research interests include physics of crystal growth, hybrid material fabrications, and photonic networking devices. Dr. Yanagiya is a member of IEEE, the Japanese Association for Crystal Growth, the Japanese Society of Applied Physics, and the Physical Society of Japan.